

Magnetic-Thrust Flexible Electrode with Integrated Preamplifier for Neural Recording

Toshihiko Noda*, Yoshiya Matsuzaka¹, SeokBeom Kim²,
Hiroaki Takehara, Kiyotaka Sasagawa, Takashi Tokuda,
Hajime Mushiake¹, Hiroshi Onodera³ and Jun Ohta

Nara Institute of Science and Technology, 8916-5 Takayama, Ikoma, Nara 630-0192, Japan

¹Tohoku University, 2-1 Seiryomachi Aoba-ku, Sendai 980-8575, Japan

²Okayama University, 3-1-1 Tsushima-naka, Kita-ku, Okayama 700-8530, Japan

³The University of Tokyo, 7-3-1 Hongo, Bunkyo-ku, Tokyo 113-8654, Japan

(Received June 30, 2015; accepted August 10, 2015)

Key words: neural recording, flexible electrode, magnetic thrust, integrated preamplifier

Flexible electrodes for use in recording neural activity were fabricated in this study, and their use was demonstrated. By using the mechanical force generated by a magnetic field, an electrode can be inserted into a tissue, and the position of the electrode can be controlled. The position and insertion path of the electrode can be controlled accurately with a high degree of freedom. No stiffer materials are required for the insertion process. A headstage amplifier, which is indispensable for low-noise recording, was hybrid-integrated with a flexible electrode. A miniaturized main amplifier that served as a second-stage amplifier was also fabricated. The magnetic controllability of the fabricated electrode was demonstrated using a phantom of a tissue. An *in vivo* experiment was also performed for the functional validation of the recording function. Local field potentials were recorded successfully as a result of the experiment.

1. Introduction

In the field of bioscience, electrophysiology measurement is one of the indispensable techniques for observing neural activity. Many types of electrodes have been developed and used to record the action potential of neurons. Tungsten needles and glass electrodes are typically used for single-channel recording. For multichannel recording, multisite electrode arrays are used. Multielectrode arrays (MEAs) are used as planar electrodes.^(1–3) For insertion purposes, needle-shaped electrodes, such as NeuroNexus arrays (i.e., Michigan Probe)^(4–7) or Utah Electrodes,^(8–10) are typically used. In most cases, these electrode devices are made of inorganic and rigid materials.

*Corresponding author: e-mail: t-noda@ms.naist.jp

Even if miniaturized electrodes can be fabricated, greater invasiveness might be an issue, especially in *in vivo* applications.^(11–14) From the perspective of invasiveness, flexible electrodes have advantages that are attributable to their being made of soft organic materials. However, these devices are too soft to insert into tissues. Position control of such devices is also difficult. Soft structures buckle easily when axial compressive stress is applied. Therefore, the insertion of needle-shaped soft structures by pushing is difficult. One approach to solving this problem is hardening the structure temporarily during the insertion process.^(15–18) However, the electrode becomes thick because of coating with a reinforcing material, even if the electrode itself is sufficiently thin. Moreover, only a straight path is allowed for insertion. It is difficult to insert an electrode via a curved path.

In this paper, we propose a novel approach to inserting a flexible electrode into a tissue using a pull-in force. A magnetic material formed in the shape of the flexible electrode generates a mechanical driving force in a magnetic field. The insertion path and position of the electrode are controlled by controlling the strength and direction of the magnetic field. No stiffeners are required in the insertion process. In this study, we fabricated magnetic-thrust flexible electrodes and demonstrated their position control. The fabricated electrodes had recording electrodes connected to an integrated headstage amplifier. A dedicated second amplifier, intended for use in *in vivo* experiments, was also fabricated. As a functional validation, an *in vivo* demonstration of neural recording was performed.

2. Device Structure and Fabrication

Figure 1 shows a schematic of the fabricated device, and Fig. 2 shows a photograph of the device. The device consisted of two blocks: a flexible electrode with a headstage amplifier and a main amplifier. A neural action potential has a weak signal; therefore, the amplification of the signal in the vicinity of the electrode is important for low-noise recording. The headstage amplifier was hybrid-integrated with the flexible electrode. An amplified signal was sent to the main amplifier through wiring and then sent to an external recorder.

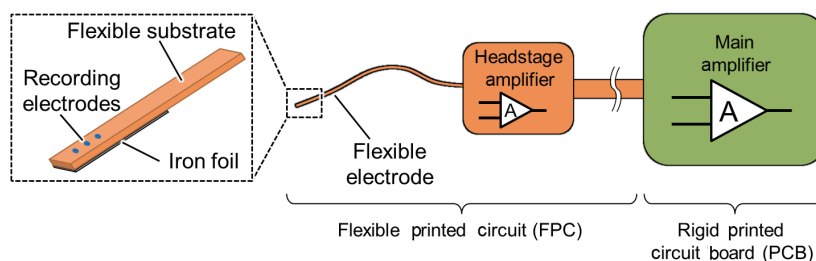


Fig. 1. (Color online) Conceptual drawing of a fabricated device.

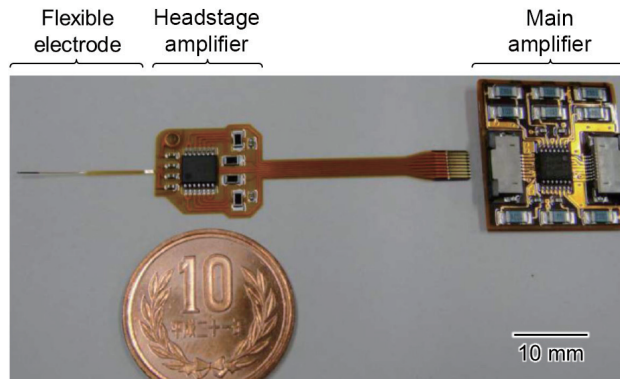


Fig. 2. (Color online) Photograph of a fabricated device.

Figure 3 shows a photograph of the flexible electrode. Recording electrodes were formed on a polyimide substrate as one part of a flexible printed circuit (FPC). The outer shape of the tip of the substrate was a needle shape that made it easy to insert the tip into a tissue. Three disk electrodes 75 μm in diameter were aligned axially with a 165 μm pitch. A 20- μm -thick pure iron foil was attached to the back side of the tip of the electrode, as shown in Fig. 4. The iron foil generated a mechanical driving force in the magnetic field.

The headstage amplifier was hybrid-integrated as the FPC with the flexible electrode, as shown in Fig. 5. A complementary metal oxide semiconductor (CMOS) rail-to-rail operational amplifier (AD8544, Analog Devices, Inc.) was used in the headstage amplifier. The headstage amplifier consisted of a four-channel preamplifier for three recording electrodes and one reference electrode. The operational amplifier and some passive elements were soldered onto the FPC. The main amplifier was fabricated on a 20 mm^2 rigid printed circuit board (PCB). A CMOS precision operational amplifier (AD8618, Analog Devices, Inc.) was used in the main amplifier. A three-channel signal from the recording electrodes was amplified differentially using a signal from the reference electrode. The signal was then amplified again for external connection to the recorder. The overall gain of the amplifier was 10000, and the frequency range was from 1 Hz to 1.8 kHz.

The fabricated device was implanted into the tissue. Therefore, the entire surface of the FPC had to be coated with biocompatible and waterproof material. Parylene-C (dichloro-di-p-xylylene) has the requisite biocompatibility⁽¹⁹⁾ and can be formed as a conformal thin film without any pinholes. Because of these properties, parylene-C was selected as the surface coating material. As a first step in the parylene coating process, the surfaces of the FPCs, which have recording electrodes and a headstage amplifier, were cleaned. The FPCs were dipped into isopropyl alcohol (isopropanol) and simultaneously irradiated ultrasonically. A surface treatment with hexamethyldisilazane

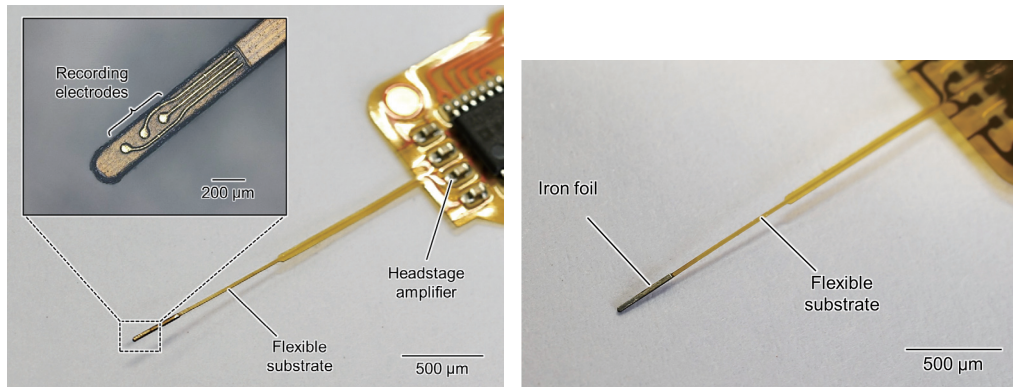


Fig. 3 (left). (Color online) Photograph of a flexible electrode. The inset shows a micrograph of the tip of the electrode.

Fig. 4 (right). (Color online) Back-side photograph of a flexible electrode.

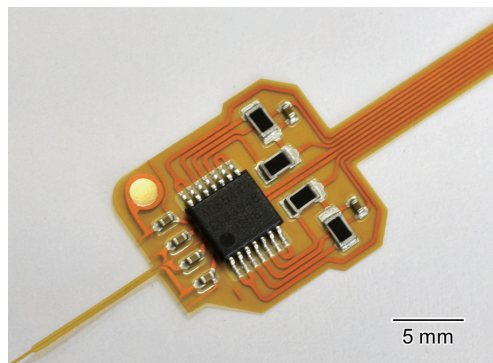


Fig. 5. (Color online) Photograph of a headstage amplifier.

(HMDS) was then performed to promote adhesion. The pretreated FPCs were loaded into a parylene-coating chamber (PDS 2010, Specialty Coating Systems, Inc.), and a 10- μm -thick parylene film was deposited onto the surfaces of the FPCs.

After the parylene coating process was completed, the parylene film covered the entire surface of each FPC, including the surfaces of the electrodes used for neural activity recording. To expose the electrode surfaces, the parylene film had to be removed from the electrodes. In this study, a laser processing technique was adopted for parylene patterning because of its flexibility in producing opening patterns of any size. A laser processing system with an yttrium aluminum garnet (YAG) laser (VL-C30, TNS Systems, LLC) was used in the patterning process. The laser beam removed the parylene film easily and could be irradiated only to the electrode region to be

opened. It was also possible to keep the electrodes covered by parylene without laser processing. The electrodes to be used for recording could be selected freely, depending on the requirements of the application, from among the electrodes on the FPC. Figure 6 shows micrographs of the tip of the FPC after the parylene coating application and laser processing were performed. Figure 6(a) shows an electrode with a parylene window 50 μm in diameter. Figure 6(b) shows an electrode with a parylene window 20 μm in diameter. The diameter of the electrode opening could be controlled by adjusting the size of the circular slit used in the laser processing.

3. Demonstration of Position Control by Magnetic Field

In this study, the magnetic properties of electrodes were measured using a high-temperature superconductor (HTS) superconducting quantum interference device (SQUID) gradiometer because the magnetic field strength of the electrodes was very small. Figure 7 shows the measured magnetic field's linear and log-scaled profiles for the iron (length = 3150 μm , width = 222 μm) attached to the pointed end of the electrode, along with the distance between the HTS SQUID gradiometer and the iron. Degaussed iron and iron magnetized by 250 mT were prepared for use as measurement samples. The magnetic field of the magnetized iron was 10 times stronger than that of the degaussed iron at short distances. Therefore, the magnetized iron was very effective in producing a large magnetic guidance force. The magnetic field strength of iron decreases proportionally to the distance between the iron and the sensor, and the relationships between the magnetic field and the distance are z^{-3} above 4 mm and z^{-2} below 4 mm.

Figure 8 shows a schematic illustration of the experiment conducted to simulate the position control of an electrode in a brain by magnetic force. A 10-mm-thick jelly dessert was used to simulate a brain. The hardness (mechanical resistance) of the jelly was measured as a preliminary experiment. Microplungers, which were 1 to 5 mm in

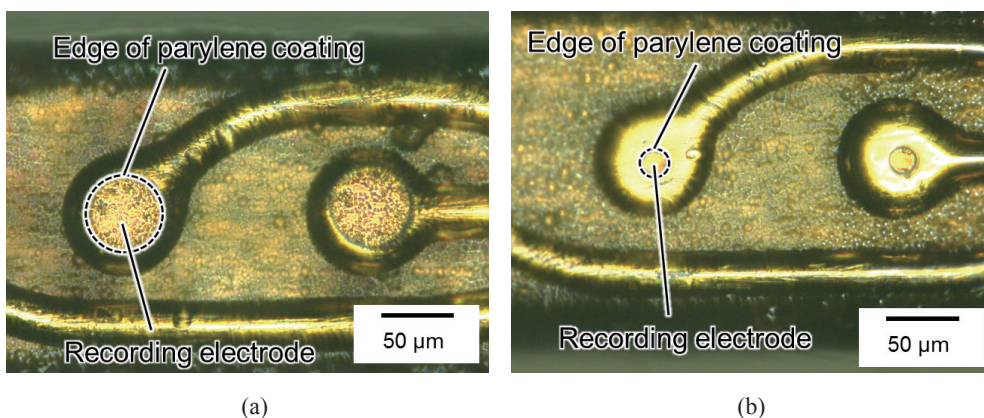


Fig. 6. (Color online) Micrographs of recording electrodes. (a) $\phi 50 \mu\text{m}$. (b) $\phi 20 \mu\text{m}$.

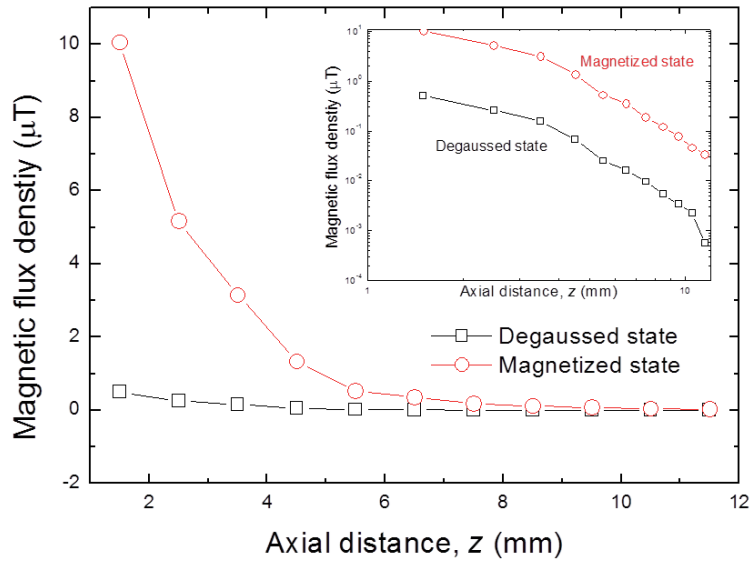


Fig. 7. (Color online) Measured magnetic field profiles of electrode by HTS SQUID gradiometer under the degaussed and magnetized states. The inset shows the log-scaled results.

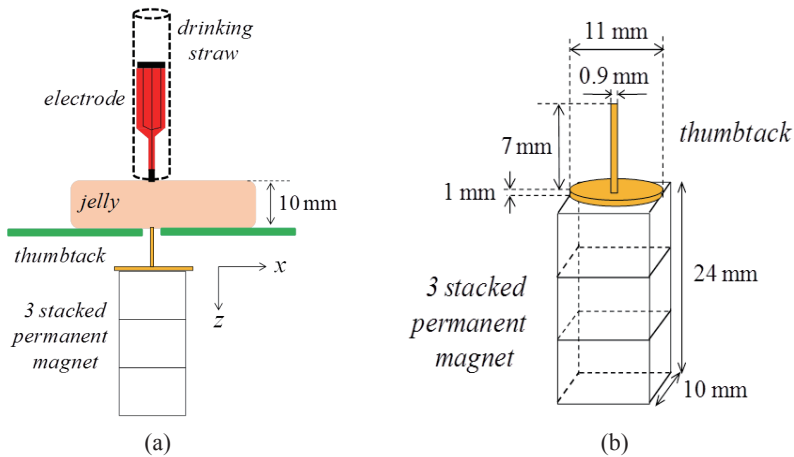


Fig. 8. (Color online) Schematic drawing of the experiment for simulating position control of the electrode in the brain by the thumbtack attached to the permanent magnet. A 10-mm-thick jelly dessert was used to simulate a brain.

diameter, were inserted into the jelly, and insertion force was measured using a texture meter. From the results of the preliminary experiment, the insertion force of a fabricated electrode was estimated at 0.8 N. The electrode was inserted into a drinking straw and positioned perpendicular to the surface of the jelly. Three stacked Nd-based permanent

magnets (PMs) were used as the source of the magnetic force, and a thumbtack was attached to the top surface of the PMs to obtain a high-gradient magnetic field, as shown in Fig. 8. The magnetic field strengths of the PMs as a function of the axial distance with and without thumbtacks were measured using a Hall sensor. Figure 9 shows typical magnetic field distributions measured at various axial distances. A high-gradient magnetic field was generated near the thumbtack, but the effect of the thumbtack was not significant when the axial distance was large.

In this study, the axial and radial distances from the pointed end of the thumbtack were used as parameters to demonstrate the position control achieved using the PMs, as shown in Fig. 10. Table 1 shows the measured distances at which position control of electrodes was possible using the PMs. These results show that position control was possible at radial distances up to 6 mm and axial distances up to 8 mm.

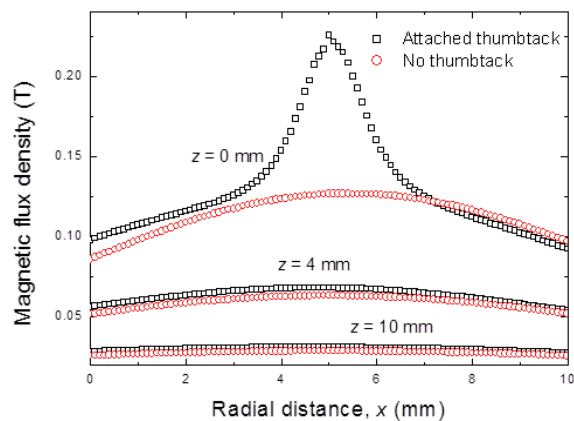


Fig. 9. (Color online) Measured typical magnetic field distributions in various axial directions.

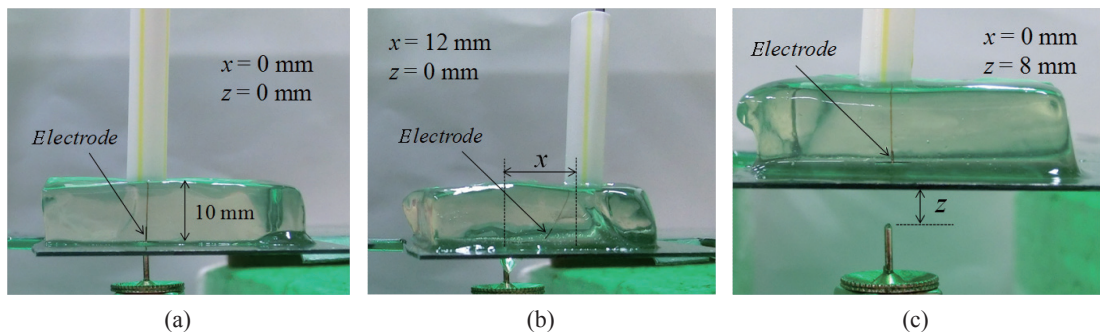


Fig. 10. (Color online) Pictures of electrode pulled at various distances by permanent magnet.

Table 1

Experimental results for position control of the electrode by magnetic field.

	$x = 0$ mm	$x = 4$ mm	$x = 6$ mm	$x = 12$ mm
$z = 0$ mm	○	○	○	×
$z = 2$ mm	○	○	×	×
$z = 4$ mm	○	○	×	×
$z = 6$ mm	○	×	×	×
$z = 8$ mm	×	×	×	×

4. Validation of Recording Function

As a functional validation of neural activity measurement, an *in vivo* experiment was performed. The *in vivo* experiment was regulated by the guidelines for animal experimentation observed at Tohoku University, Japan. A wild-type Wistar rat [body weight (b.w.) = 400 g] was used for the *in vivo* test of the electrode. The rat was housed in a solitary cage and treated in accordance with the institutional guidelines for animal experiments.

4.1 Surgery

While the rat was under anesthesia consisting of a mixture of ketamine (10 mg per 100 g b.w.) and xylazine (0.1 mg per 100 g b.w.), the rat's head was held in a stereotaxic apparatus. The head was shaved, and xylocaine was injected subcutaneously. The head skin was then incised to expose the skull. A small opening (3 to 4 mm in diameter) was made in the skull over the right primary sensory cortex. Three screws were attached to the skull surrounding the opening. These screws later served as grounds as well as anchors for a protective cap.

4.2 Neuronal activity recording

Prior to the implantation of the flexible electrode, we examined the sensory receptive field under the opening. For this purpose, we recorded the neuronal activity in the underlying cortex using glass-insulated elgiloy electrodes (impedance = 1 M Ω at 1 kHz). The somatosensory receptive fields were monitored on an oscilloscope by tapping, brushing the skin, and manipulating the limb joints.

Once the receptive fields were identified, a flexible electrode was attached to a manually driven electrode manipulator (Narishige SM-12) and advanced into the cortex. The electrode was stabilized by attaching it to the skull using dental acrylic. The built-in headstage amplifier was connected to a secondary amplifier. The neural activity was amplified (gain = 10000) and filtered using a Butterworth filter (two poles, pass band = 1 Hz–1.8 kHz), and digitized by an analog-to-digital (AD) converter (Measurement Computing, USB-1208HS) at 1 kHz to record the local field potential (LFP). The neural activity data were stored on a hard disk for later offline analysis.

4.3 Analysis

The sensory responses recorded during the experiment were analyzed offline. During the resting period, when no stimuli were applied to the animal, we looked for the presence of slow oscillation and beta synchronization. During the application of somatosensory stimulation, we investigated whether there was any activity modulation synchronized with the stimulation and whether the modulation was evoked by the selective stimulation of the receptive field, as confirmed by the prior recording with the metal electrodes.

4.4 Results

We recorded the response of the LFP to somatosensory stimuli through a flexible electrode inserted into the brain of an anesthetized rat. The electrode was inserted into the right somatosensory cortex (2 mm posterior from the bregma and 2 mm from the midline). Prior to the insertion of the flexible electrode, neuronal activity recording was conducted using a metal electrode, and it was ascertained that the neurons in this region had a somatosensory receptive field in the right hindlimb region.

Figure 11 illustrates the LFP signal recorded through the flexible electrode. During the resting period in which no somatosensory stimuli were applied, the LFP exhibited clear spindle oscillation.⁽²⁰⁾ When somatosensory stimuli were applied to the hindlimb,

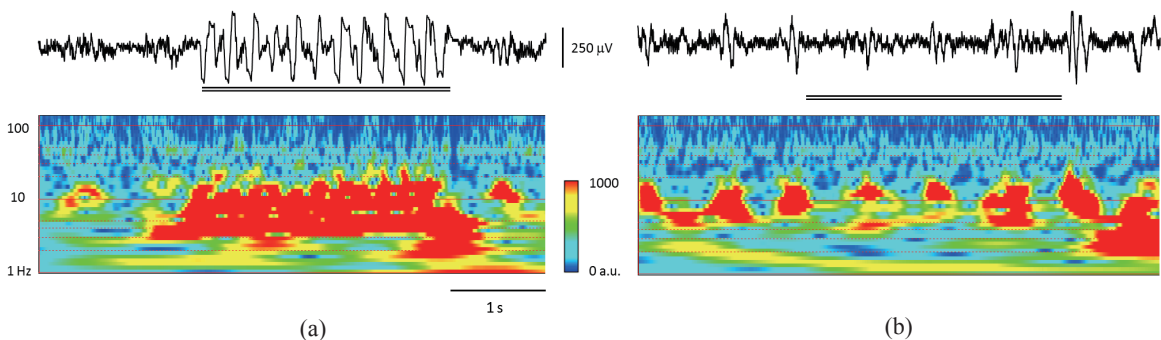


Fig. 11. LFPs recorded from an anesthetized rat's somatosensory cortex. Both the raw waveform and its wavelet transformation are shown. Preliminary recording using a metal electrode showed that the neurons in this region had a somatosensory receptive field on the left hindlimb. (a) LFP and its response to the tapping applied to the receptive field. The double line represents the time period during which the stimulation was applied. Prior to the recording, the LFP intermittently exhibited spindle oscillation that lasted several hundred milliseconds (frequency = 10 Hz). During the somatosensory stimulation, it responded with a large-amplitude fluctuating activity that was synchronized with the tapping. (b) LFP and its response to the somatosensory stimulation applied out of the receptive field (left vibrissae). The LFP continued to exhibit periodic spindle oscillation, but no somatosensory response was evoked.

the LFP responded with a repeating fluctuation synchronized with the tapping [Fig. 11(a)]. The absence of such a response when a somatosensory stimulus was applied out of the receptive field confirmed that the observed response was the somatosensory response of the local neurons rather than merely contact noise [Fig. 11(b)].

5. Conclusions

In this study, a flexible electrode with an integrated headstage amplifier was fabricated, and its use was demonstrated. Because an iron foil was attached to the tip of the electrode, a mechanical force that pulled the flexible electrode in was generated in the magnetic field. Accurate control of the electrode position with a high degree of freedom of the insertion path was possible. Magnetic positioning of the electrode was successfully demonstrated using a material used to simulate brain tissue. A low-noise headstage amplifier and a main amplifier were also fabricated. Because the output of the main amplifier could be connected directly to an external recorder, compact amplifiers were found to be useful and convenient in the animal experiment conducted. The recording function of the fabricated devices was successfully demonstrated through an *in vivo* experiment.

The elements of the proposed device were successfully validated, and the entire system, i.e., electrode insertion into an animal's brain by the application of a magnetic field and the recording of neural activity, can be expected. The magnetic-thrust electrode developed in this study will become a powerful tool in the field of bioscience.

Acknowledgements

Part of this study was supported by a Grant-in-Aid for Scientific Research (A), #26249051, from the Ministry of Education, Culture, Sports, Science and Technology (MEXT) of Japan. This study was also supported by the CREST program "Creation of novel technology towards diagnosis and treatment based on understanding of molecular pathogenesis of psychiatric and neurological disorders" of the Japan Science and Technology Agency.

References

- 1 C. Thomas, Jr., P. Springer, G. Loeb, Y. Berwald-Netter and L. Okun: *Exp. Cell Res.* **74** (1972) 61.
- 2 G. W. Gross, E. Rieske, G. W. Kreutzberg and A. Meyer: *Neurosci. Lett.* **6** (1977) 101.
- 3 U. Egert, D. Heck and A. Aertsen: *Exp. Brain Res.* **142** (2002) 268.
- 4 D. J. Anderson, K. Najafi, S. J. Tanghe, D. A. Evans, K. L. Levy, J. F. Hetke, X. L. Xue, J. J. Zappia and K. D. Wise: *IEEE Trans. Biomed. Eng.* **36** (1989) 693.
- 5 R. J. Vetter, J. C. Williams, J. F. Hetke, E. A. Nunamaker and D. R. Kipke: *IEEE Trans. Biomed. Eng.* **51** (2004) 896.
- 6 K. Najafi, K. D. Wise and T. Mochizuki: *IEEE Trans. Electron Devices* **32** (1985) 1206.
- 7 J. D. Weiland and D. J. Anderson: *IEEE Trans. Biomed. Eng.* **47** (2000) 911.

- 8 P. K. Campbell, K. E. Jones, R. J. Huber, K. W. Horch and R. A. Normann: *IEEE Trans. Biomed. Eng.* **38** (1991) 758.
- 9 P. J. Rousche and R. A. Normann: *IEEE Trans. Rehabil. Eng.* **7** (1999) 56.
- 10 S. Kim, R. Bhandari, M. Klein, S. Negi, L. Rieth, P. Tathireddy, M. Toepper, H. Oppermann and F. Solzbacher: *Biomed. Microdevices* **11** (2009) 453.
- 11 P. J. Rousche and R. A. Normann: *J. Neurosci. Methods* **82** (1998) 1.
- 12 R. Biran, D. C. Martin and P. A. Tresco: *Exp. Neurol.* **195** (2005) 115.
- 13 V. S. Polikov, P. A. Tresco and W. M. Reichert: *J. Neurosci. Methods* **148** (2005) 1.
- 14 R. Zhu, G. L. Huang, H. Yoon, C. S. Smith and V. K. Varadan: *J. Nanotechnol. Eng. Med.* **2** (2011) 031001.
- 15 S. H. Felix, K. G. Shah, V. M. Tolosa, H. J. Sheth, A. C. Tooker, T. L. Delima, S. P. Jadhav, L. M. Frank and S. S. Pannu: *J. Visualized Exp.* **79** (2013) e50609.
- 16 F. Barz, P. Ruther, S. Takeuchi and O. Paul: *Proc. 28th IEEE Int. Conf. Micro Electro Mechanical Systems (MEMS)* (2015) pp. 636–639.
- 17 P. R. Patel, K. Na, H. Zhang, T. D. Y. Kozai, N. A. Kotov, E. Yoon and C. A. Chestek: *J. Neural Eng.* **12** (2015) 046009.
- 18 S. Felix, K. Shah, D. George, V. Tolosa, A. Tooker, H. Sheth, T. Delima and S. Pannu: *Annu. Int. Conf. IEEE Eng. Med. Biol. Soc.* **2012** (2012) 871.
- 19 B. D. Winslow, M. B. Christensen, W.-K. Yang, F. Solzbacher and P. A. Tresco: *Biomaterials* **31** (2010) 9163.
- 20 D. Contreras, A. Destexhe, T. J. Sejnowski and M. Steriade: *J. Neurosci.* **17** (1997) 1179.